Molecular Engineering of Cyanine Dyes to Design a Panchromatic Response in Co-sensitized Dye-Sensitized Solar Cells: Electronic Supplementary Information

Giulio Pepe[a], Jacqueline M. Cole[a,b,*], Paul G. Waddell[a,c,†], Scott McKechnie[a]

[a] *Cavendish Laboratory, University of Cambridge, J. J. Thomson Avenue, Cambridge, CB3 0HE, UK*

[b] *Argonne National Laboratory, 9700 S. Cass Avenue, Argonne, IL 60439, USA.*

[c] *Australian Nuclear Science and Technology Organisation Lucas Heights, New South Wales, 2234, Australia*

* *E-mail: jmc61@cam.ac.uk (J. M. Cole)*

Table of Contents

1 Current address: School of Chemistry, Newcastle University, Newcastle upon Tyne, NE1 7RU. UK.

S.1 X-Ray Diffraction

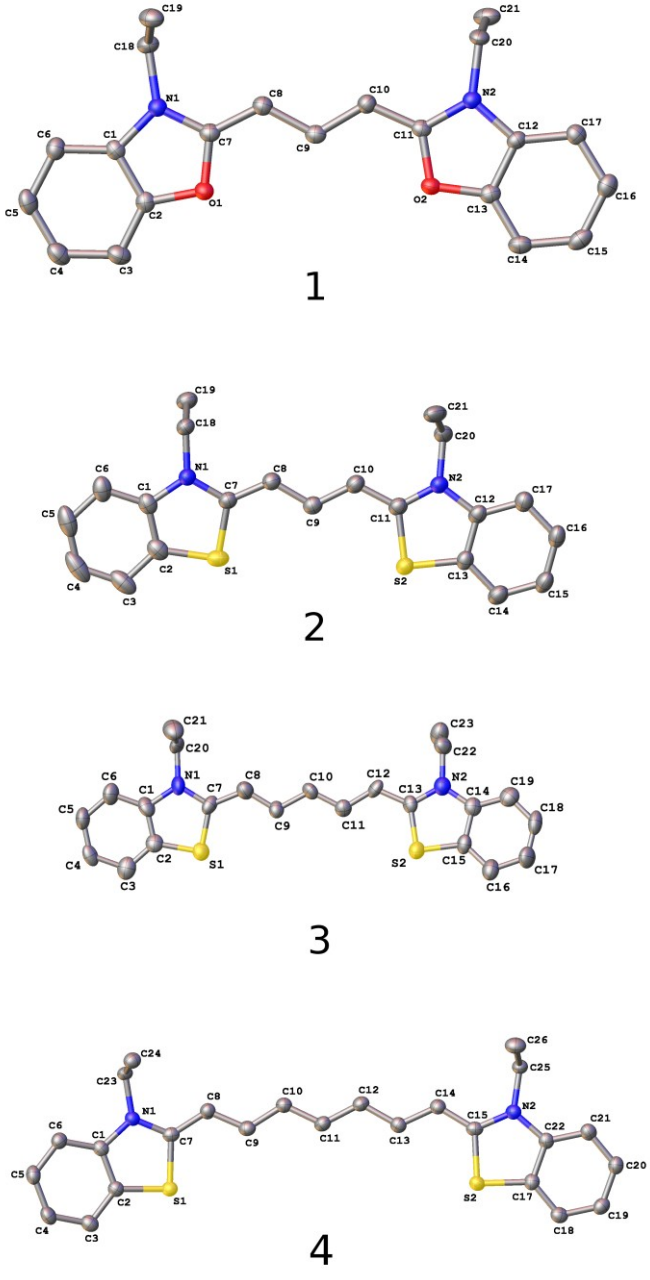

Figure S1: The asymmetric units of the crystal structures of parent dyes **1-4**. Atomic displacement ellipsoids are drawn at the 50% probability level. The iodide counter-ion and all hydrogen atoms have been omitted for clarity.

S.2 UV/vis absorption spectroscopy

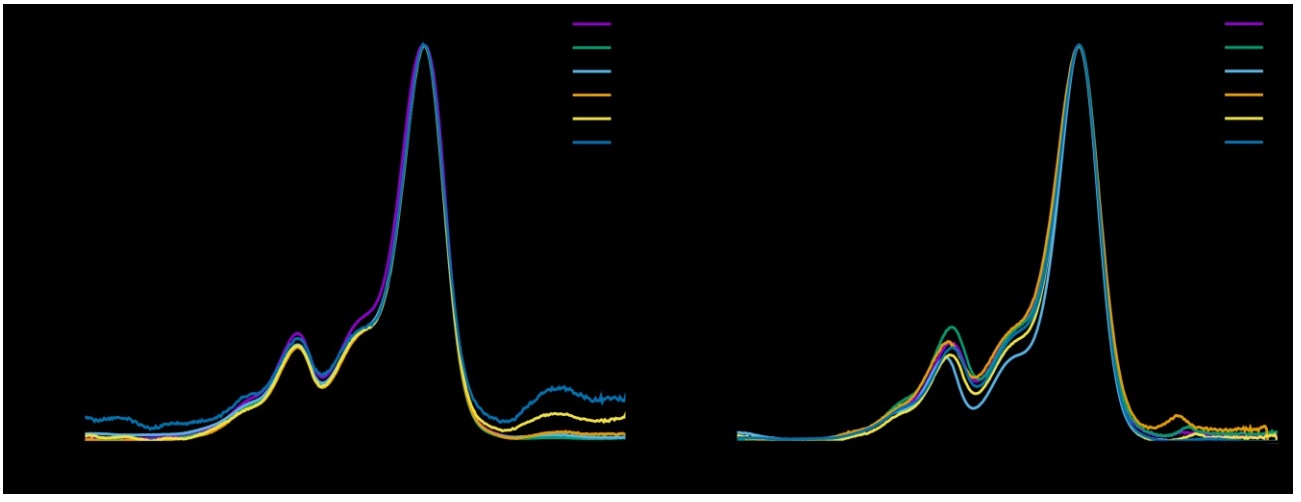

Figure S2: (Left) Experimental absorption spectrum of **3** in methanol at different concentrations. The curves have been normalized to the maximum absorption for easier comparison. (Right) Experimental absorption spectrum of **3** in different solvents at 0.0156 mM. The curves have been shifted (with acetone as reference) and normalized to the maximum absorption for easier comparison.

S.3 Cyclic Voltammetry

The HOMO energy of each dye can be derived from their cyclic voltammograms by analyzing the onset potential of the oxidation peak:

$$E_{HOMO} = E_{[onset,oxidation\ vs.\ vacuum]}$$

The onset oxidation potential is a measure dependent to the reference electrode, Ag/AgCl.

The conversion to vacuum can be carried out by shifting the voltage with respect to the standard hydrogen electrode (SHE) as reference:

0 [V] vs. Ag/AgCl(3M KCl @ 20C) = 0.21 [V] vs. SHE

The SHE reference can be converted to absolute electrode potential according to:[1]

0 [V] vs. vacuum = 4.281 [V] vs. SHE

This value has to be corrected for the liquid junction potential in acetonitrile, which results in subtracting 0.093 V from the conversions with respect to the SHE and Ag/AgCl.[2]

Therefore, the HOMO energy can be calculated as:

E_{HOMO} [eV] = - ($E_{[onset,oxidation\ vs.\ Ag/AgCl]}$ + 4.398) [eV]

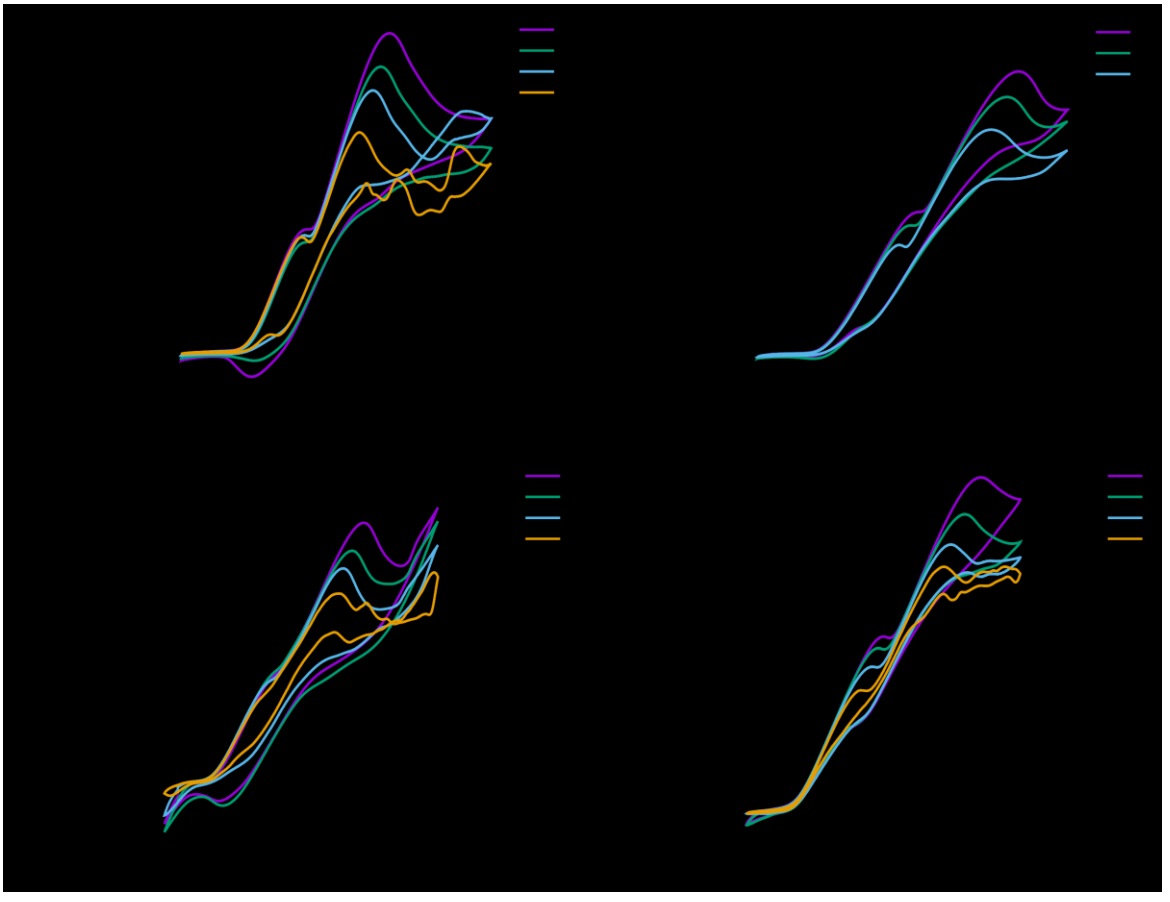

Figure S4: Cyclic voltammograms of **1-4** (1 mM) in acetonitrile at different scanning speeds: 100, 75, 50, 25 mV/s. (a), (b), (c), (d) correspond to **1**, **2**, **3**, **4**, respectively.

S.4 Quantum chemistry studies

S.4.1 Benchmarking the effect of counter-ion on parent dyes, 1-4

Compounds	ΔE_V (B3LYP) [eV]	ΔE_V (CAM-B3LYP) [eV]	RMSD (PBE1PBE) [Å]
1	0.00	0.00	0.09
2	0.02	0.03	0.08
3	0.03	0.03	0.05
4	0.01	0.02	0.07

Table S1: Study of the effect of the iodide counter-ion on the geometries and energies calculated using DFT and TD-DFT with PCM (methanol). Difference in lowest-vertical excitation energies and RMSD deviations are calculated for parent dyes **1-4** between the geometrically optimized dye containing and lacking the counter-ion. The presence of the iodide counter-ion does not significantly affect geometries and energies.

S.4.2 Benchmarking models of theory on parent dyes, 1-4

Computational calculations on organic dyes with a push-pull architecture are known to produce compromised estimations of vertical excitation energies, when using non long-range corrected functionals. The calculated energies show a consistent overestimation of the true π-π* excitation, largely present in organic dyes.[3,4] Cyanines have been long known to perform badly in TD-DFT calculations with most functionals.[5] Despite the highly delocalized electrons in the polymethine chain, the use of nonhybrid GGA PBE or the long-range corrected CAM-B3LYP [6] did not lead to a significantly closer agreement to wave function methods. In fact, all TD-DFT functionals largely overestimated the vertical excitation energies. A recent study [7] on cyanine dyes using the M06 family of Minnesota density functionals [8] showed an agreement with diffusion Monte Carlo (DMC) of ΔE = 0.1-0.2 eV, when using the high Hartree–Fock exchange functional M06-HF. We report similar results on **1-4** in the gas phase for this functional, using EOM-CCSD calculations as the reference. Despite the high correlation of results between the experimentally measured lowest-vertical excitation energies and M06-HF, the functional overestimated the excitation energies by ΔE = 0.51 eV on average. The inclusion of implicit solvent (PCM) effects reduced the overestimation to ΔE = 0.35 eV. Similar results, in methanol, were reported for the Becke's three-parameter and Lee–Yang–Parr hybrid functional (B3LYP).[9] Although the electron delocalization on the polymethine chain suggests high values of intra-molecular charge transfer, the orbital-overlap measure (Λ) introduced by Tozer and co-workers [10, 11] for **1-4** was 69% < Λ < 71% for all dyes. This is a low orbital-overlap threshold value (Λ < 40%) that indicates inaccuracies for local functionals and suggests the use of long-range corrected functionals. In fact, the overestimation of CAM-B3LYP was ΔE = 0.45 eV on average for **1-4** in solution.

All TD-DFT calculations were performed for 8 excitations and the 6-311+G(2d,p) basis set was used with a PCM solution model in methanol. Yet, discrepancies between experimental results are still significant with all functionals tested. In-house benchmarks on a

large set of molecules over different TD-DFT and coupled-cluster methods have shown that LT-DF-LCC2 is a feasible model for small organic molecules, providing accurate results in absolute energies. The low-lying vertical excitation energies, E_V, were calculated using LT-DF-LCC2 with extended domains and cc-pVTZ auxiliary basis sets (JKFIT and MP2FIT).[12,13] Solvent effects were included by subtracting the difference between the single-excitation CI (CI-Singles) calculation on excited states for the molecule in the gas phase and in methanol (PCM) from the LCC2-calculated excitation energy. CI-Singles calculations reduced the overestimation from experiments to $\Delta E = 0.15$ eV, on average, making LCC2 methods the most accurate model to calculate E_V in cyanine dyes.

Following a similar procedure, DFT calculations were performed on chemical derivatives of **1-4**, computationally designed to (i) include two types of anchoring groups: carboxylic acid and cyanoacrylic acid at different chemical substitution positions, and (ii) change the length of the central polymethine chain. The geometry of each new engineered molecule was optimized and single-point DFT was performed at the same level of theory as for the parent dyes. For benchmarking purposes, TD-DFT calculations were performed using B3LYP, CAM-B3LYP and M06-HF with the 6-311+G(2d,p) basis set. Lowest-vertical excitation energies were calculated using LT-DF-LCC2 with extended domains, as described for the parent dyes.

	B3LYP	**M06-HF**	**EOM-CCSD**
1	3.12 (3.04)	3.24 (3.16)	3.09
2	2.75 (2.69)	2.79 (2.72)	2.64
3	2.50 (2.45)	2.44 (2.39)	2.26
4	2.27 (2.23)	2.16 (2.11)	1.95
RMSD	0.21	0.17	-
Correlation	99.89%	99.97%	-

Table S2: Benchmark of the lowest-vertical excitation energies for different models of theory for **1-4**. TDDFT(B3LYP/6-311+G(2d,p)) and TDDFT(M06-HF/6-311+G(2d,p)) functionals have been tested against EOM-CCSD, in gas phase. In order to solve problems of convergence and reduce the cost of EOM-CCSD calculations, the methyl groups anchored on the N atom have been replaced with a hydrogen atom for all calculations. Lowest-vertical excitation energies for the TDDFT studies including the methyl group are reported in brackets. It can be noted that these energies vary within 0.1 eV from the hydrogen-replaced molecules, as the methyl group does not play a role in the excitation of the molecule. Root-mean-squared-deviations (RMSD) and correlations between TD-DFT studies and EOM-CCSD are reported. M06-HF was the best performing functional, considering the higher correlation and smaller deviations from the coupled-cluster studies.

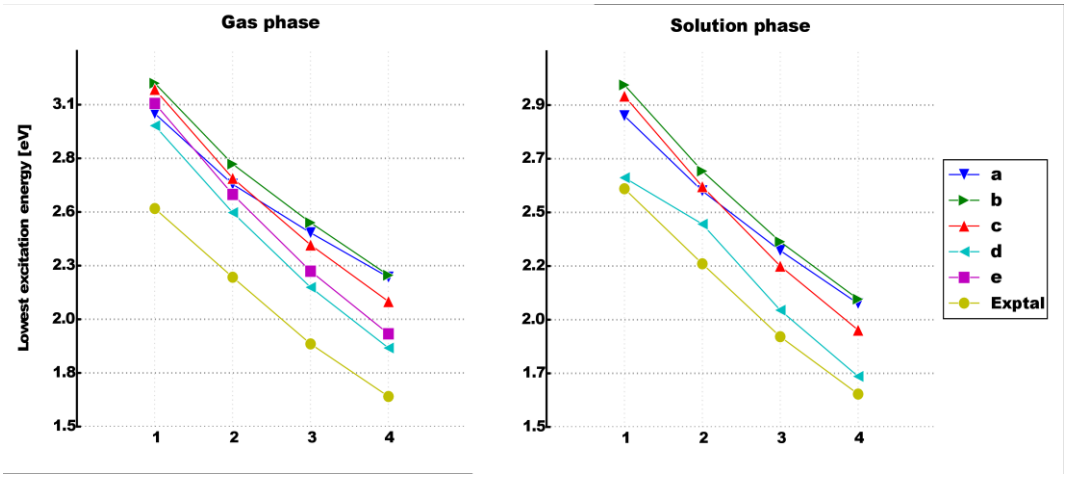

Figure S5: Lowest-vertical excitation energies (calculated and experimental) for **1-4** for different models of theory in gas phase (left) and solution phase (right): a, B3LYP; b, CAM-B3LYP; c, M06-HF; d, LT-DF-LCC2; e, EOM-CCSD.

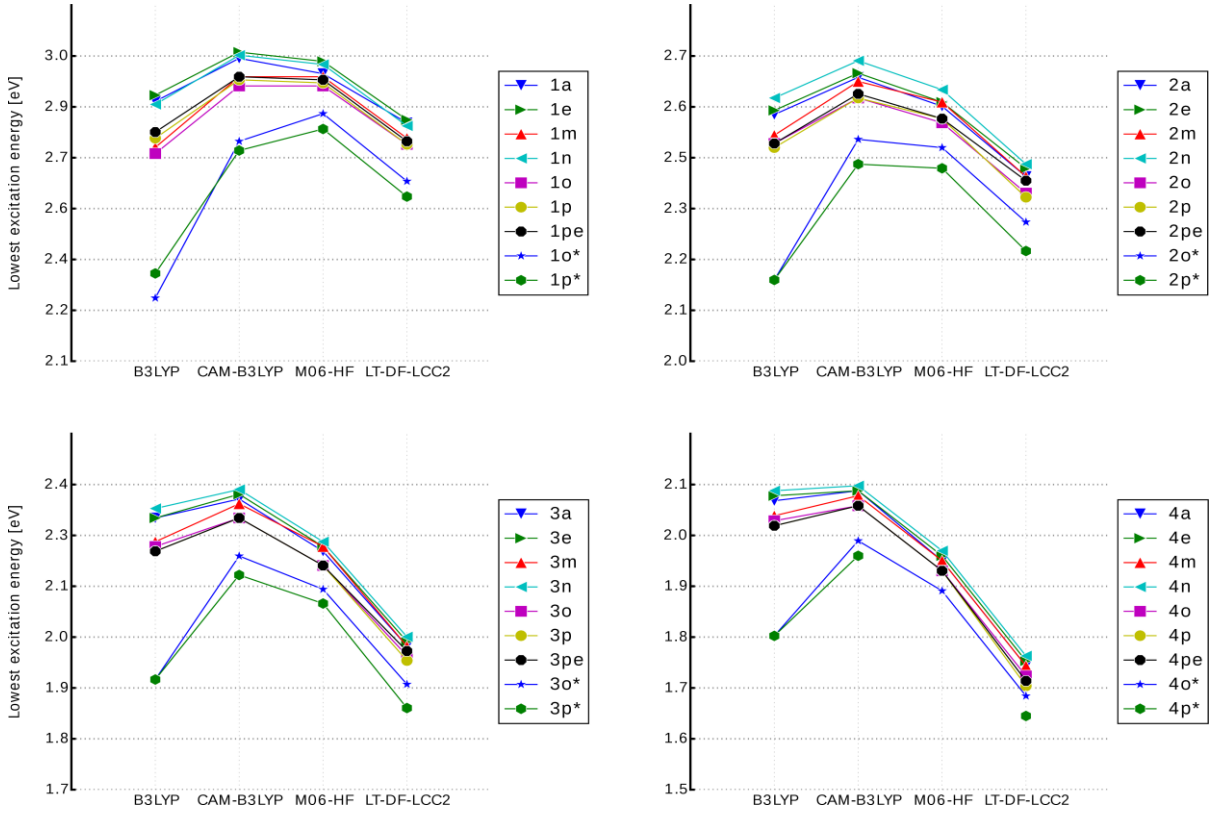

Figure S6: Benchmark of TD-DFT functionals for E_V in the molecular engineering of the anchoring groups. The four plots refer to the four parent dyes and each data point is a derivative for three different functionals B3LYP, CAM-B3LYP and M06-HF with LT-DF-LCC2 as reference model. There is a clear overestimation of TD-DFT compared to LCC2 for all functionals. Overestimations are not consistent, most likely due to the nature of the functionals (long-range correction or different amount of HF exchange). Inconsistencies between different molecules show that the way each functional calculates the excitation energies is heavily affected by the charge transfer processes in the molecule. In support of this, the cyanoacrylic acid substitutions, which have an unusually large electron density on the anchors, have the largest deviations between different models. All calculations were performed in methanol solution (PCM) at the 6-311+G* level of theory.

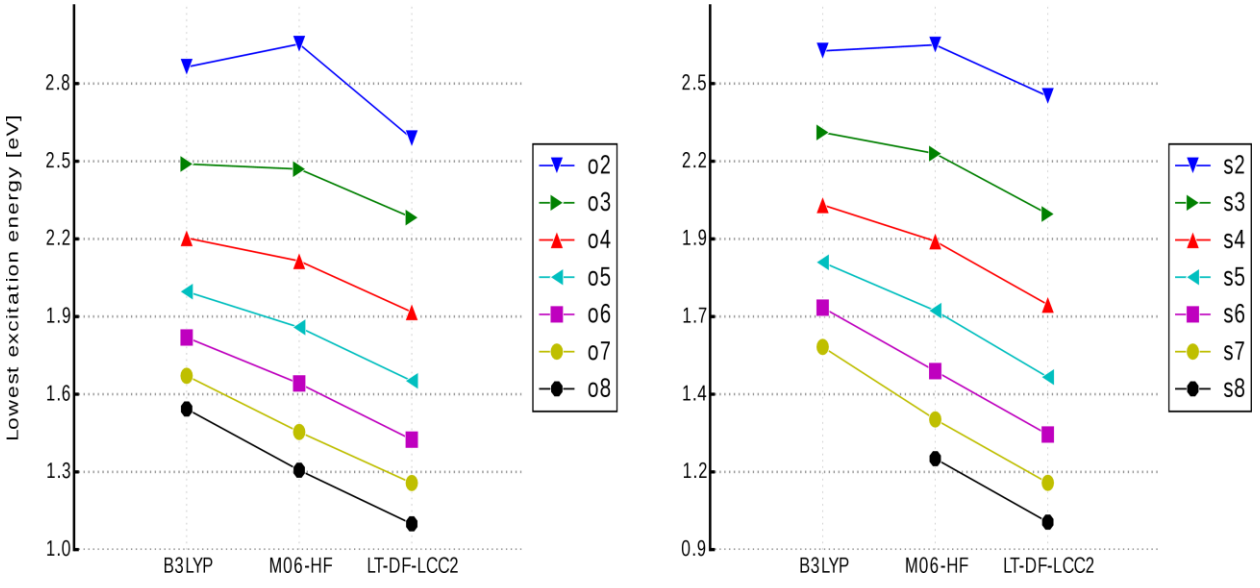

Figure S7: Benchmark of TD-DFT functionals for E_V in the molecular engineering of the polymethine chain. Each data point is a derivative for two different functionals B3LYP, M06-HF and LT-DF-LCC2 as reference model. There is a clear overestimation of the vertical excitation energy by TD-DFT. Biggest deviations between the models are reported for the shortest methine chains. All calculations were performed in methanol solution (PCM) at the 6-311+G* level of theory.

	B3LYP	CAM-B3LYP	M06-HF	EOM-CCSD	LT-DF-LCC2	B3LYP*	CAM-B3LYP*	M06-HF*	LT-DF-LCC2*	Experimental*
1	3.04	3.19	3.16	3.09	2.98	2.90	3.04	2.99	2.62	2.57
2	2.69	2.79	2.72	2.64	2.55	2.56	2.65	2.58	2.41	2.23
3	2.45	2.50	2.39	2.26	2.18	2.29	2.33	2.22	2.02	1.90
4	2.23	2.24	2.11	1.95	1.88	2.05	2.07	1.93	1.72	1.64
RMSD	0.52	0.59	0.51	0.41	0.32	0.37	0.44	0.35	0.12	-
Correlation(%)	99.74	99.82	99.83	99.95	99.97	99.93	99.92	99.96	98.92	-

Table S3: Benchmark of different models of theory compared to experimental values for **1-4**. Starred models indicate that the result is for the molecules in solution (methanol). TD-DFT studies employed functionals with different amounts of Hartree-Foch exchange: B3LYP, CAM-B3LYP, M06-HF, using the 6-311+G(2d,p) basis set. As previous studies have shown, the best performing TD-DFT functionals for molecules with high orbital overlap ($\Lambda > 70\%$ for **1-4**) are the ones without the long-range correction. The calculations in solution were performed by applying PCM. EOM-CCSD calculations were performed on the molecules substituted with a hydrogen instead of the methyl groups to accelerate convergence. Solution effects in LT-DF-LCC2 were provided by an energy shift calculated using the difference between the single-excitation CI (CI-Singles) calculation on excited states for the molecule in gas phase and in methanol (PCM). Experimental results were calculated from UV/vis absorption studies. Root-mean-squared-deviations (RMSD) and correlations between the calculations and the experimental results are reported. Despite its smaller correlation, LT-DF-LCC2 was the best performing functional compared to experiments.

S.4.3 Computational modeling of derivatives of 1-4

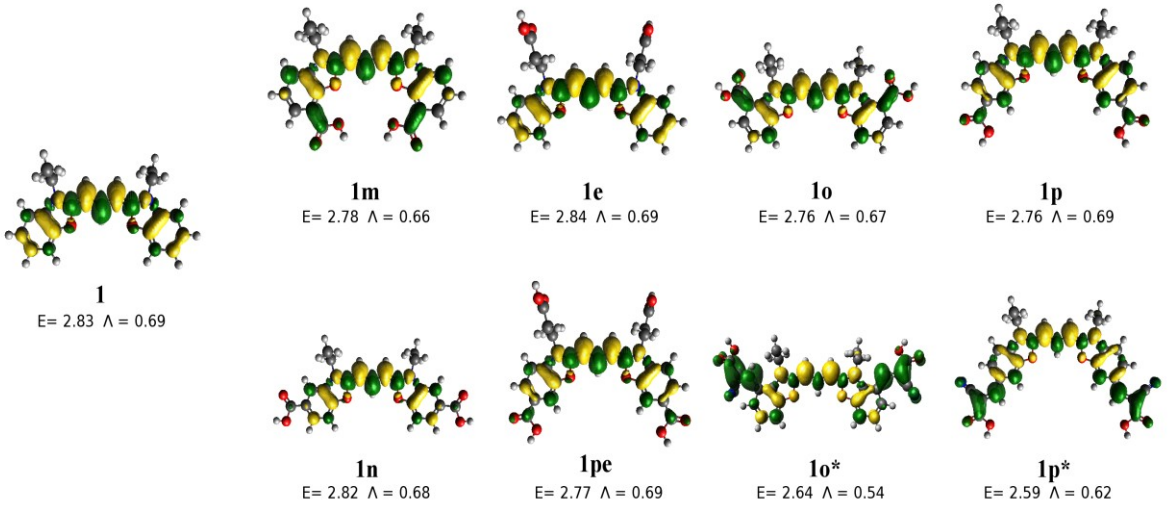

Figure S8: Difference density orbitals, $LUMO^2$-$HOMO^2$, of derivatives of **1** generated from DFT calculations at the PBE1PBE level of theory with 6-311+G(2d,p) basis set and PCM. Increasing electron density is represented in green, while decreasing electron density is represented in yellow. The vertical excitation energies, E_V, (in eV) and the spatial orbital overlaps, Λ, are annotated.

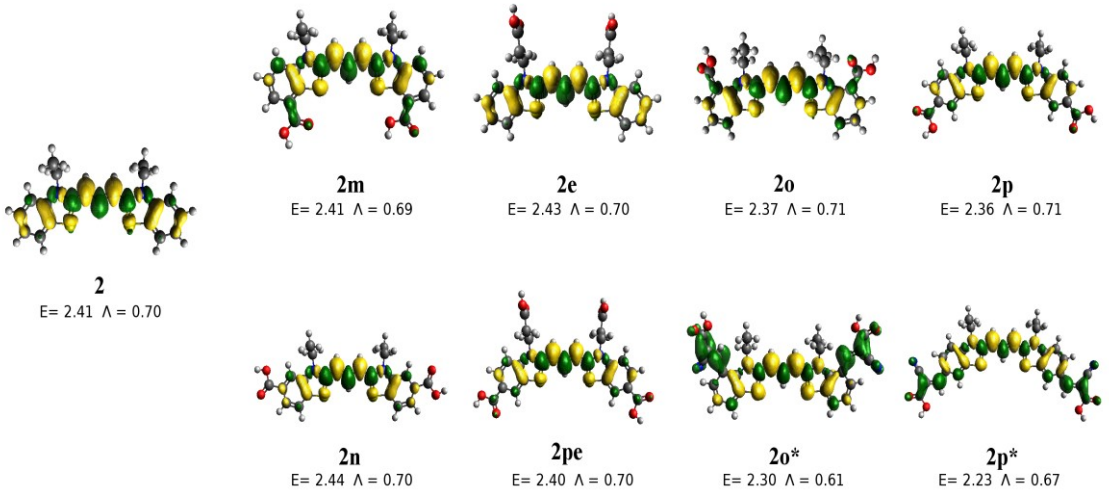

Figure S9: Difference density orbitals, $LUMO^2$-$HOMO^2$, of derivatives of **2** generated from DFT calculations at the PBE1PBE level of theory with 6-311+G(2d,p) basis set and PCM. Increasing electron density is represented in green, while decreasing electron density is represented in yellow. The vertical excitation energies, E_V, (in eV) and the spatial orbital overlaps, Λ, are annotated.

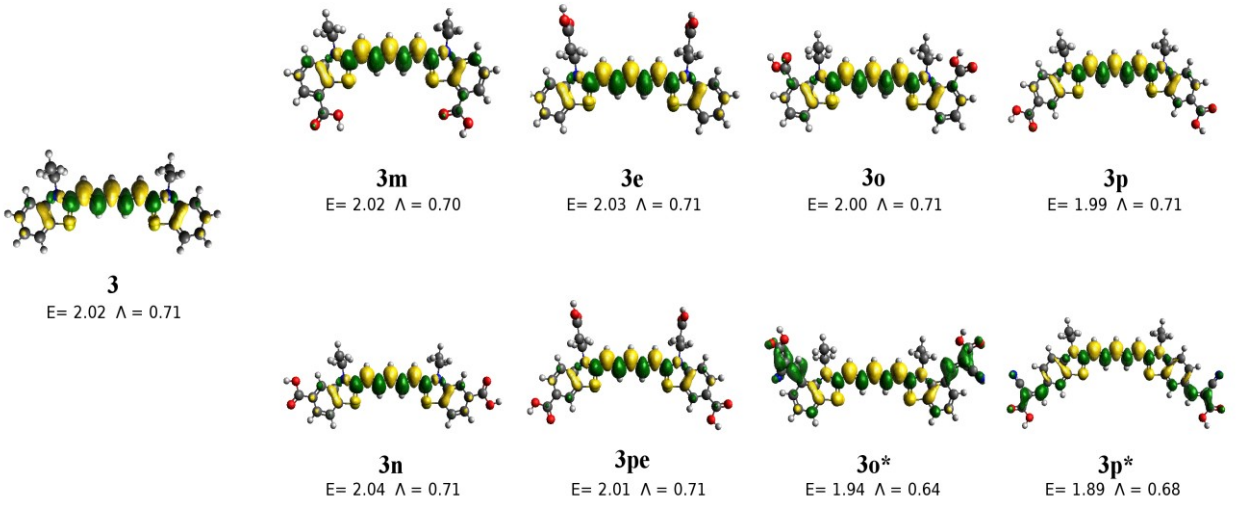

Figure S10: Difference density orbitals, $LUMO^2$-$HOMO^2$, of derivatives of **3** generated from DFT calculations at the PBE1PBE level of theory with 6-311+G(2d,p) basis set and PCM. Increasing electron density is represented in green, while decreasing electron density is represented in yellow. The vertical excitation energies, E_V, (in eV) and the spatial orbital overlaps, Λ, are annotated.

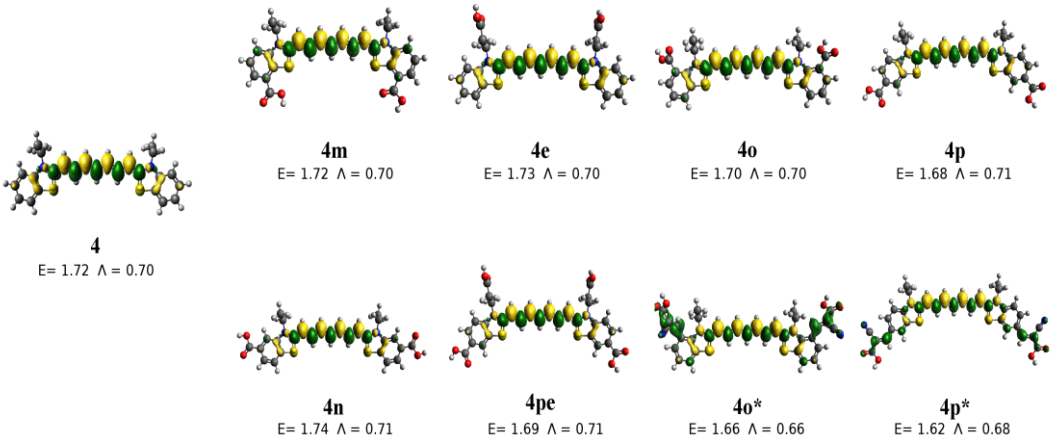

Figure S11: Difference density orbitals, $LUMO^2$-$HOMO^2$, of derivatives of **4** generated from DFT calculations at the PBE1PBE level of theory with 6-311+G(2d,p) basis set and PCM. Increasing electron density is represented in green, while decreasing electron density is represented in yellow. The vertical excitation energies, E_V, (in eV) and the spatial orbital overlaps, Λ, are annotated.

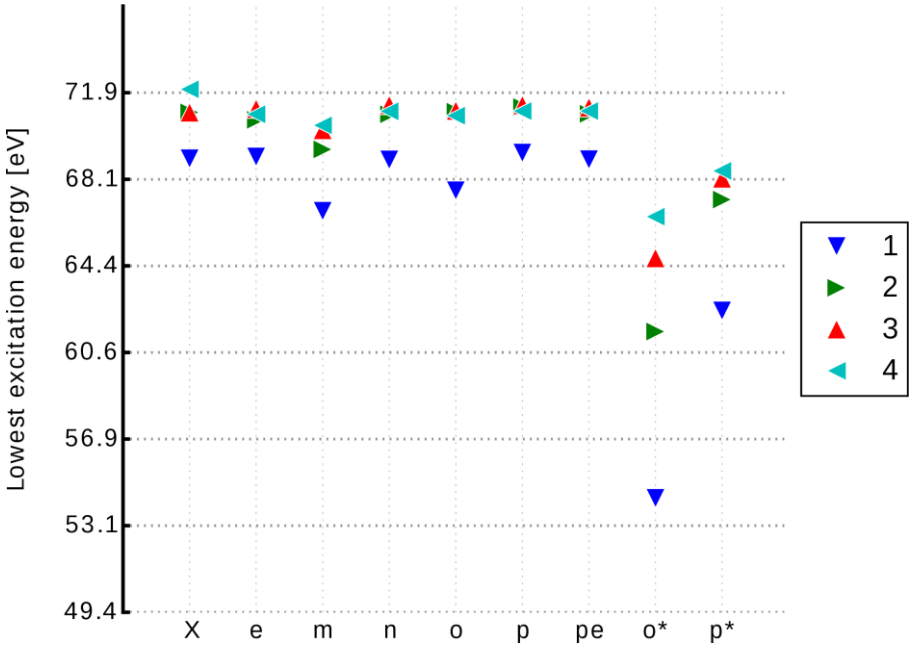

Figure S12: Value of the spatial orbital overlap, Λ, for derivatives of **1-4** engineered with an anchoring group at different positions. **X** refers to the parent dye. **e** (ethylene), **m** (meta-1), **n** (meta-2), **o** (ortho) and **p** (para) involve addition of the carboxylic acid anchoring group (COOH) at the indicated positions. **pe** involves the addition of COOH at both **p** and **e** positions. **o*** and **p*** are respectively the ortho- and para- substitutions of cyanoacrylic acid as anchoring group.

S.4.4 $(TiO_2)_9$ cluster atomic positions

Atom	x-position	y-position	z-position
Ti	15.6181	4.915257	15.538679
Ti	14.656039	6.531828	13.34211
Ti	17.613459	6.270851	13.08594
Ti	14.907321	7.679475	15.89544
Ti	20.75371	6.862666	12.242809
Ti	18.144937	4.270597	15.519405
Ti	20.762607	5.138394	14.77007
Ti	17.901846	7.483138	15.838273
Ti	21.136004	8.061333	15.539596
O	14.320878	4.940144	14.100751
O	16.506931	3.427434	16.089748
O	15.998929	6.52309	12.119939
O	16.415538	8.474763	16.506535
O	13.865553	7.895651	14.349067
O	14.579851	6.088665	16.664016
O	21.360157	5.298375	13.036662
O	17.128385	4.584195	13.950862
O	19.874559	3.641029	15.478823
O	19.05209	5.949794	14.72939
O	21.668387	6.23336	15.834641
O	18.97042	6.233881	11.96149
O	17.978321	8.085584	13.904925
O	20.702593	8.038422	13.60583
O	17.393451	5.716852	16.531218
O	22.237354	9.17945	15.984697
O	19.397398	8.19721	16.403101
O	16.051565	6.719305	14.671194

Table S4: Initial atomic positions for DFT geometry optimization of the $(TiO_2)_9$ slab

References and Notes

1 A. A. Isse, A. J. Gennaro, *Phys. Chem. B*, 2010, **114**, 7894.
2 J. W. Diggle, A. J. Parker, *Aust. J. Chem.*, 1974, **27**, 1617.
3 D. Jacquemin, *et al.*, *J. Chem. Theory Comput.*, 2008, **4**, 123.
4 D. Jacquemin, A. Planchat, C. Adamo, B. Mennucci, *J. Chem. Theory Comput.*, 2012, **8**, 2359.
5 D. Jacquemin, V. Wathelet, E. A. Perpete, C. Adamo, *J. Chem. Theory Comput.*, 2009, **5**, 2420.
6 T. Yanai, D. P. Tew, N. C. Handy, *Chemical Physics Letters*, 2004, **393**, 51.
7 D. Jacquemin, *et al.*, *J. Chem. Theory Comput.*, 2012, **8**, 1255.
8 Y. Zhao, D. G. Truhlar, *Theor Chem Account*, 2007, **120**, 215.
9 C. Lee, W. Yang, R. G. Parr, *Physical Review B,* 1988, **37**, 785.
10 M. J. G. Peach, P. Benfield, T. Helgaker, D. J. Tozer, *J. Chem. Phys.*, 2008, **128**, 044118.
11 M. J. Peach, D. J. Tozer, *Journal of Molecular Structure: THEOCHEM*, 2009, **914**, 110.
12 F. Weigend, *Phys. Chem. Chem. Phys.*, 2002, **4**, 4285.
13 F. Weigend, A. Kohn, C. Hattig, *J. Chem. Phys.*, 2002, **116**, 3175.